European Review for Medical and Pharmacological Sciences 2022; 26: 2847-2860

Low expression of integrin signaling pathway genes is associated with abdominal aortic aneurysm: a bioinformatic analysis by WGCNA

G.-M. CAO, X.-Z. XUAN, H.-L. DONG

Department of Vascular Surgery, The Second Hospital of Shanxi Medical University, Taiyuan, Shanxi, China

Genmao Cao and Xuezhen Xuan contributed equally to this work

Abstract. – OBJECTIVE: An abdominal aortic aneurysm (AAA) is a potentially fatal disease associated with a high risk of rupture. AAA is pathologically distinguished by atherosclerotic thrombosis, immune cell infiltration, smooth muscle cell apoptosis, and extracellular matrix degradation. Given that there are no effective target treatments, once ruptured, AAA leads to high mortality with few long-term survivors. The goal of this study is to identify novel key pathways and hub genes involved in AAA formation with the aim of providing promising therapeutic targets for AAA.

MATERIALS AND METHODS: The transcriptome sequencing matrix of GSE47472 and GSE57691 were obtained from the GEO database. These datasets were further merged for differential expression analysis, weighted gene co-expression network analysis (WGCNA), and functional enrichment analysis in R (v4.0.2). A co-expression network was constructed with Cytoscape (v3.8.0) to generate the top 30 hub genes. Hub Genes with high clinical traits and potential values were further verified using a receiver operating characteristic (ROC) curve and qPCR analysis.

RESULTS: A total of 745 differentially expressed genes were screened and 14 gene co-expression modules were established. Among these 14 modules, pink modules with a total of 118 genes showed the strongest correlation with AAA pathogenesis. Subsequently, 78 genes associated with a highly relevant clinical trait and the top 30 hub genes were intersected to generate 22 genes. Gene ontology functional enrichment analysis of the 22 genes revealed abnormal expression of genes relating to cell-matrix adhesion and integrin-mediated signaling pathway. *LAMA5, ITGA8, ITGA1*, and *FERMT2* were associated with the integrin-mediated signaling pathway and cell-matrix adhesion while *ACTN1* and *CX3CL1* were simply associated with the latter. Low expressions of *LAMA5, ACTN1, ITGA8, ITGA1,* and *FERMT2* were further verified through qPCR in a mouse model of AAA.

CONCLUSIONS: Low expression of partial genes in the integrin signaling pathway was implicated in the function loss of mediated cell-matrix adhesion, which may offer novel targets for therapeutic intervention against AAA.

Key Words:
WGCNA, Abdominal aortic aneurysm, Adhesion gene.

Introduction

Abdominal aortic aneurysm (AAA) refers to the permanent dilation (> 50%) of the abdominal aorta from the diaphragm to the common iliac artery[1]. As the most common type of life-threatening aneurysms, AAA is more likely to occur in men, smokers, and in the elderly. Population-based ultrasound screening studies have shown that AAA occurs in 4-7% of men aged 65 or older and in 1-2% of women[2]. The vascular wall structure of a dilated abdominal aorta is vulnerable and is apt to spontaneous rupture, which may rapidly lead to death. The risk of AAA rupture increases with diameter. Even after receiving emergent treatment, the 3-year mortality rate following an AAA rupture remains at 48% for endovascular repair and 56% for open repair[3]. However, during the past 20 to 30 years, mortality after an AAA has decreased significantly in Western countries, mainly due to the government control of tobacco[4].

The underlying mechanisms of AAA pathology are multifactorial, relating to environmental, genetic, and biochemical factors. The main pathological manifestations include atherosclerotic thrombosis[5], immune cell infiltration, smooth muscle cells apoptosis, and extracellular matrix (ECM) degradation[6]. Destruction of aortic wall integrity is the principal cause of AAA. Matrix metalloproteinases (MMPs) can promote degradation of the ECM in AAA. Studies[7] have shown that expression of MMP-1,

Corresponding Author: Honglin Dong, MD, Ph.D; e-mail: honglindong@sxmu.edu.cn

-2, -3, -9, -12, and -13 was upregulated in AAA tissue by the JNK and JAK/stat signaling pathways, resulting in the degradation of collagen, elastin, ECM glycoprotein, and proteoglycan in the aortic wall. Although high expression of ADAMTS-1 in AAA[8] and ADAM-17 in the endothelium and adventitia of the aorta[9] has been reported, it remains unclear yet whether other family members of disintegrins and metalloproteinases with the thrombospondin motifs (ADAMTs) are involved in AAA formation. Low density lipoprotein receptor-associated protein 1 (LRP1) is an important component involved in maintenance of the aortic wall integrity through regulation of HTRA1 and connective tissue growth factor[10]. Deletion of LRP1 in the vascular smooth muscle cells (VSMCs) can aggravate AngII-induced ascending aortic aneurysms[11]. In AAA, VSMCs can switch from a contractile (healthy) state to a synthetic (diseased) state, triggering excessive ECM production, aortic sclerosis, and pro-inflammatory signaling molecules. The transforming growth factor-β (TGFβ) signaling pathway is the chief mechanism involved in the synthesis of extracellular matrix protein, elastin, and collagen in the aorta. Studies[12] have shown that TGF-β is protective for AAA formation.

Weighted gene co-expression network analysis (WGCNA) is a commonly used bioinformatic method, which can be used to identify gene clusters with similar expression patterns and to link gene expression profiles to clinical characteristics[13]. In this study, we sought to identify central modules and hub genes for AAA through WGCNA analysis, and to further validate our findings *in vivo*. Our findings may advance the understanding of AAA pathogenesis and aid identification of novel therapeutic targets.

Materials and Methods

Data Sources

The human abdominal aortic aneurysm transcriptome sequencing dataset was downloaded from GEO (Gene Expression Omnibus) database. GSE47472 (containing 14 AAA samples and 8 normal abdominal aorta samples) and GSE57691 (including 49 AAA samples and 10 normal abdominal aorta samples) were downloaded and analyzed for differentially expressed genes (DEGs). GSE47472 and GSE57691 were sequenced on the Illumina HumanHT-12 V4.0 Expression BeadChip (GPL10558) platform. The experimental groups in the datasets contained specimens of human AAA while the control groups contained samples of donated normal abdominal aorta. All data analyses were processed on R (v4.0.2).

DEG Analysis

Raw files were first processed using the Limma package. The merged expression matrices of the two chips were processed with RemoveBatchEffect function to remove the batch effect. The screening criteria for DEGs were false discovery rate (FDR) <0.05 and log of fold change (logFC) >0.6.

Construction of Co-Expression Network

Genes with the top 20% median absolute deviation (MAD) value were filtered to identify the co-expression network. The expression matrix was checked by GoodSamplesGenes function for missing values. Subsequent cluster analyses and cluster tree diagrams were conducted and generated, respectively, to check for outliers. An appropriate soft threshold power β was generated using the pickSoft threshold function in the WGCNA R package to ensure a scale-free network.

GO Enrichment Analysis

Gene Ontology (GO) enrichment analysis was performed using Clusterprofiler package[14] for the genes within modules and DEGs. GO analysis was conducted in three aspects: biological processes (BP), cellular components (CC), and molecular functions (MF). p-values <0.05 were deemed to be statistically significant. This study focused on genes with high connectivity correlating to clinical traits in each module.

Hub Gene Screening and Efficacy Evaluation

As the first principal component of each module, module eigengenes (MEs) feature the expression pattern of the whole module. Pearson correlation coefficient was computed between MEs and sample characteristics to reveal key modules with clinical significance. Correlation coefficients > 0.3 and p-values < 0.05 were validated as the thresholds of screening key modules. Gene significance (GS) refers to the Pearson correlation coefficient value between gene expression and the corresponding phenotype. Module membership (MM) refers to the Pearson correlation coefficient value between MEs and certain gene expressions. GS represents the connectivity between gene and phenotype, while MM represents the connectivity between gene and module. GS and MM are highly linked in the identification of hub genes.

Genes with |MM| > 0.8 and |GS|> 0.2 were selected and imported into Cytoscape (v3.8.0) to construct a co-expression network. The Cytohubba plugin identified the top 30 hub genes within the network. Subsequently, receiver operating characteristic (ROC) curves were plotted to yield area under the curve (AUC) values using the pROC package. Genes with an AUC > 0.7 were considered valuable for predicting which would be useful for further verification by qPCR experiments.

Generating a Mouse Model of AAA

Male C57/BL6J mice aged 8-10 weeks (purchased from laboratory animal center of Shanxi Medical University) were anesthetized with ether inhalation. First, a ventral midline incision was made through the abdominal skin and muscles. Intraperitoneal organs (mainly the colon) were exposed and gently pushed to the right side, covered with wet gauze soaked in 0.9% (v/v) saline. The fascia surrounding the inferior vena cava and abdominal aorta was carefully located and dissected to avoid venous injury and significant bleeding. Gelatin sponge (1 mm * 1 mm * 5 mm) dipped in elastase solution (100 mg/ml) was then placed on the infrarenal aorta for 20 minutes. The control group was treated with a gelatin sponge dipped in 0.9% (v/v) saline. After removing the sponge, peritoneal lavage was performed with 0.9% (v/v) saline at 37°C three times. Muscle and skin were sutured with 6-0 nylon sutures following reset of abdominal organs. Mice were placed on a heating pad for recovery post-surgery. Mice were fed by 0.2% (v/v) 3-aminopropionitrile fumarate (BAPN). Development of AAA was confirmed through laparotomy 7 days later. The model was considered to be successful if the diameter of aneurysm increased by more than 50%.

Validation of Hub Genes

Quantitative Polymerase Chain Reaction (qPCR) was used to detect expression of hub genes in the mouse model. Mice were sacrificed 7 days post-surgery and the abdominal aorta was carefully separated from connective tissue on the surface, making sure to avoid injury to the arterial adventitia. Mice were transcardially perfused with 0.9% (v/v) saline. Blood samples were collected from the abdominal artery lumen for total RNA extraction. RNA was extracted using the Tiangen RNA Simple Total RNA Kit. Subsequently, reverse transcription was conducted with extracted total RNA (1 μg) using PrimeScript RT Master Mix (RR036A, Takara). Amplification was performed using SYBR Green Premix (RR420A, Takara). NADPH was used as the internal reference. A Kolmogorov-Smirnov test was used to validate the normality of data distribution and an independent-sample *t*-test was used to validate any significant differences between the AAA and sham groups using the ΔΔCT method. *p*-values < 0.05 were considered statistically significant. The study cascade is illustrated in Figure 1 and qPCR primers used in this work are listed in Table I.

Results

DEG Analysis

Profiles of GSE47472 (including 14 AAA samples and 8 aorta donor samples) and GSE57691 [including 49 AAA samples, 9 aortic occlusive disease (AOD) samples, and 10 aorta donor samples] were downloaded. The profiles of the AOD samples in GSE57691 were deleted. Following preprocessing and standardization, an expression matrix of 81 samples and 19,140 genes was eventually acquired. The cluster dendrogram was constructed based on cluster analysis on all samples (Figure 2A). The height of threshold was set as 50 and no outlier samples were detected. Therefore, all samples were included in the subsequent analysis. Subsequently, 745 DEGs were filtered through differential expression analysis, which resulted in the identification of 83 up- and 662 downregulated genes (Figure 2B, C).

Co-Expression Network

When the threshold of the Pearson correlation coefficient was set at |±0.9|, average connectivity reached the highest at a soft-thresholding power of 4 (Figure 3A). We constructed 14 co-expression modules using the blockwise Modules function (min module size = 30, deep split = 3) (Figure 3B). The turquoise module contained the most co-expressed genes (1506 DEGs), followed by the blue module with 1016 DEGs. All 14 modules have mutually independent functions (Figure 3C).

Key Module and Hub Genes

The association between each module and clinical features (AAA formation) was evaluated by GS of MEs. The pink module showed high association with AAA formation ($p = 4 \times 10^{-5}$) (Figure 4A). The pink module is hereafter referred to as the key module in subsequent analyses (Figure 4B). Next, 78 out of 114 genes were filtered as

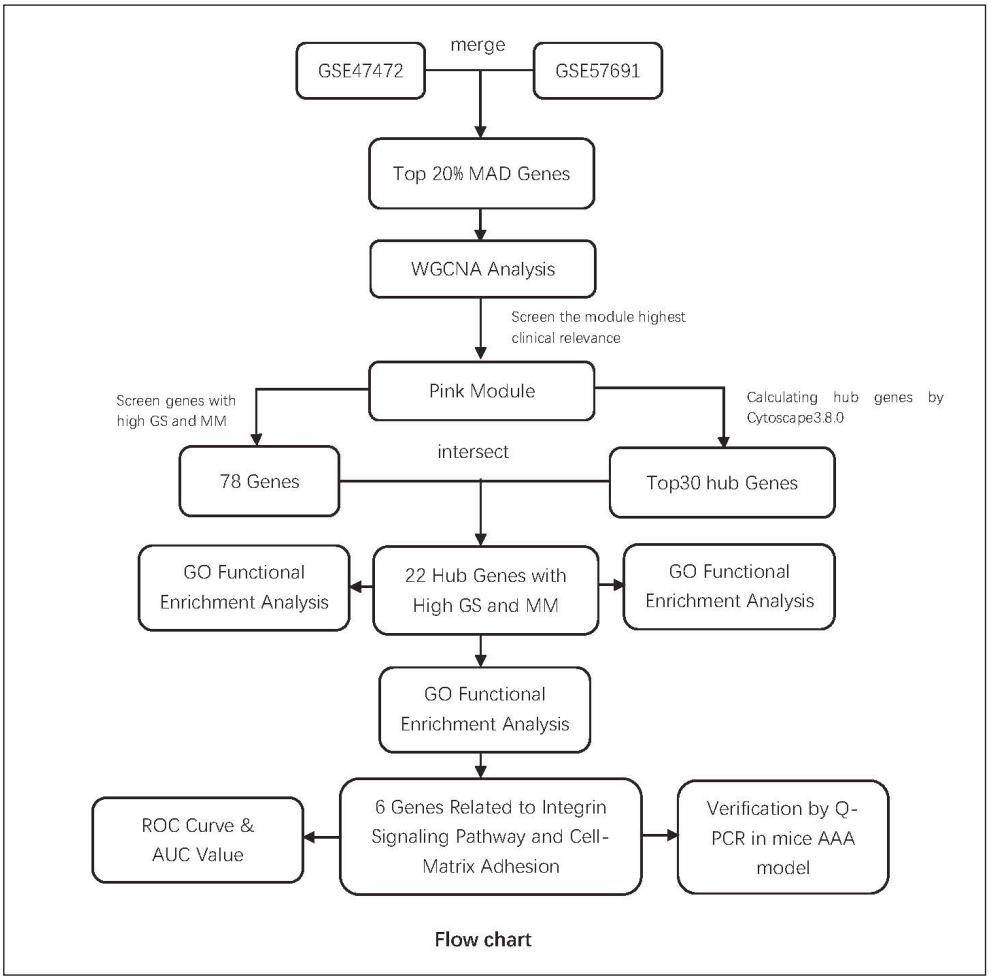

Figure 1. Study cascade illustrating how genes were screened and which analyses were conducted.

|GS|> 0.2 and |MM| > 0.8 in the pink module. A topological overlap matrix TOM plot was generated and it showed strong internal intercorrelations among the 78 genes (Figure 4C). Genes in the pink module were imported into Cytoscape (v3.8.0) using the exportNetworkToCytoscape function (threshold=0.1) to construct a co-expression network. The top 30 hub genes in the network were identified using Plugin Cytohubba (MNC) (Figure 5C).

Table I. Primers used in Q-PCR.

Genes	Sequences
Actn1-F	GGTCATCTCAGGTGAACGCTTGG
Actn1-R	ACCCCTTTGCTGGCTATGAAATCC
Fermt2-F	TGGACGGGATAAGGATGCCA
Fermt2-R	TGACATCGAGTTTTTCCACCAAC
Itga8-F	CGAAGCCGAACTCTTTGTTATCA
Itga8-R	GGCCTCAGTCCCTTGTTGT
Itga1-F	CCTTCCCTCGGATGTGAGTCA
Itga1-R	AAGTTCTCCCCGTATGGTAAGA
Lama5-F	GCGTGTGTTTGACCTACACCA
Lama5-R	GGTCTCGATGAGTTGGGCTG
Cx3cl1-F	ACGAAATGCGAAATCATGTGC
Cx3cl1-R	CTGTGTCGTCTCCAGGACAA

GO Functional Enrichment Analysis

GO enrichment was conducted for 78 trait-related genes as well as for the top 30 hub genes. We found that 78 trait-related genes were mainly enriched in (1) muscle cell proliferation, differentiation, and development; (2) adhesion/junctions between cells and the matrix, and focal adhesion; (3) actin binding, actin filament binding, and actinin binding (Figure 5A). The top 30 hub genes were mainly enriched in (1) cell-matrix adhesion and focal adhesion; (2) actin binding and actin filament organization; and (3) the integrin-mediated signaling pathway (Figure 5B). Subsequently, 22 genes were identified through intersection of 78 trait genes and

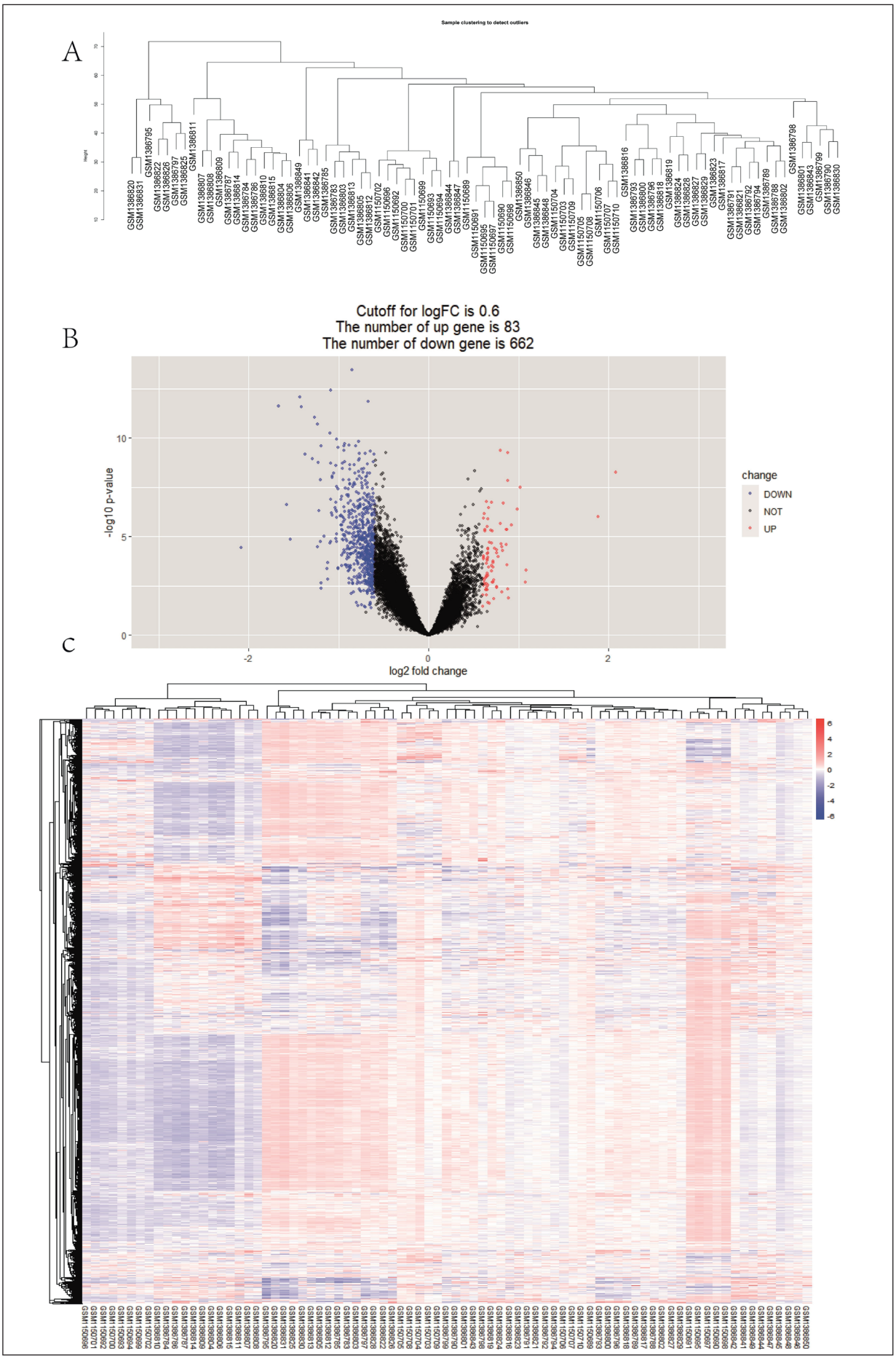

Figure 2. ***A,*** Cluster analysis for all AAA samples and donor aorta samples indicated no outliers. ***B,*** Volcano plot of differential expression analysis showed that downregulated genes were significantly fewer than upregulated genes. ***C,*** Heatmap of all genes. From blue to red, the color illustrates the transition from low to high gene expression, respectively.

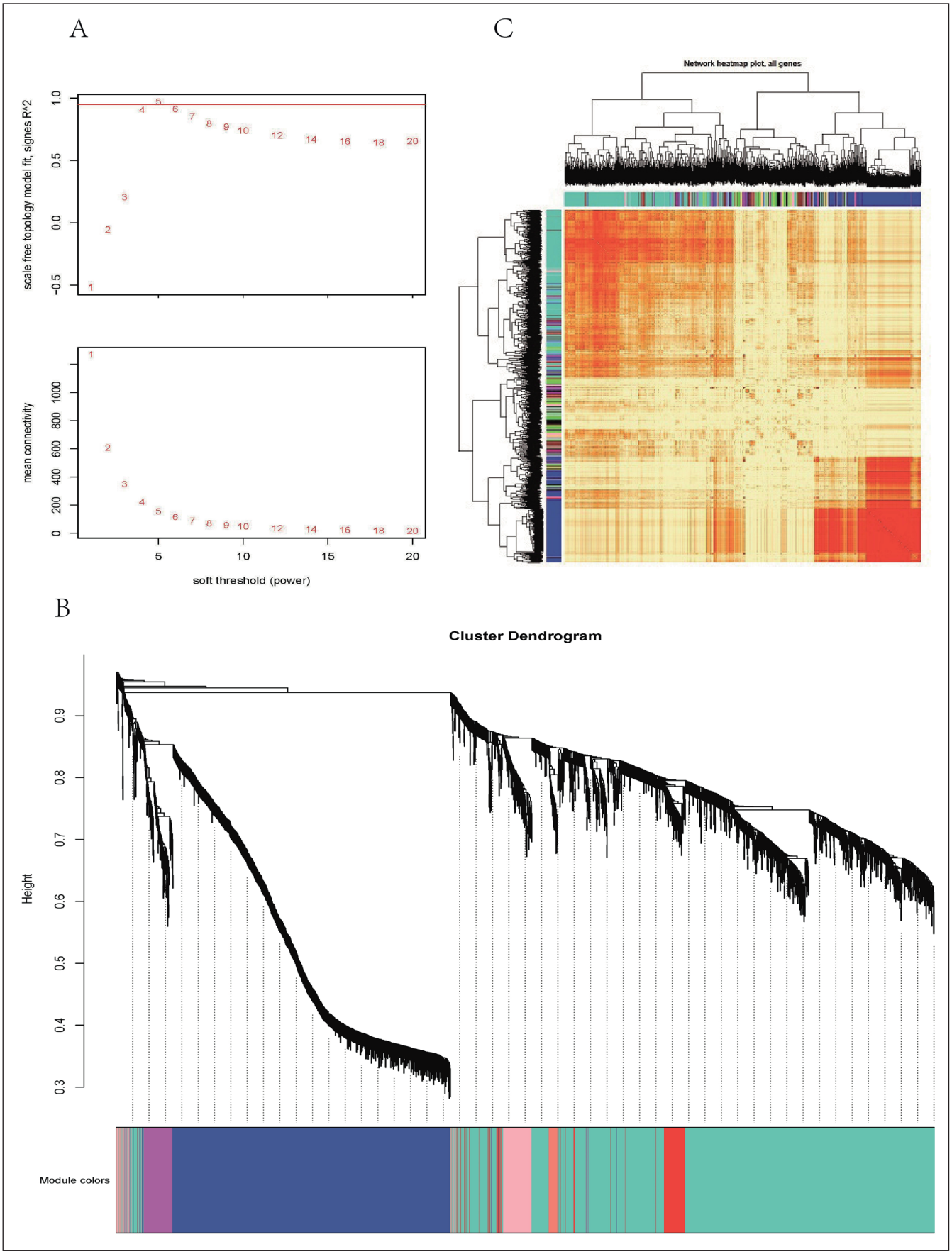

Figure 3. A, Plot of different soft-thresholding powers from one to twenty and their corresponding scale-free fit index and mean connectivity. When soft-thresholding power equaled 4, the scale-free fit index was > 0.9 and mean connectivity reached the maximum. ***B,*** Clustering dendrogram of genes with top 20% MAD in AAA and aorta tissue. ***C,*** TOM plot of 14 co-expression modules (the intensity of the red indicates the strength of the correlation between modules).

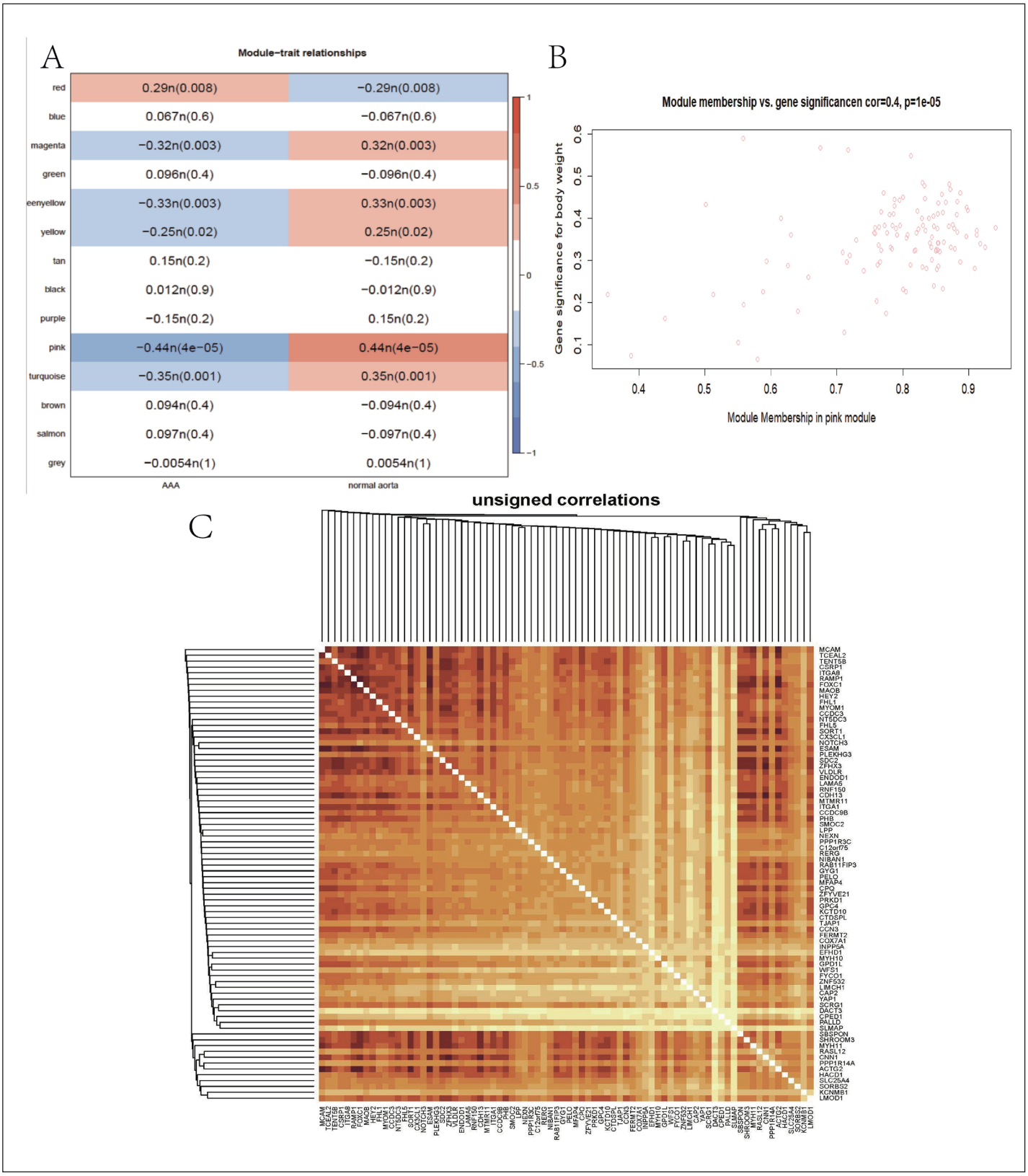

Figure 4. A, Heatmap of correlation between modules and AAA/normal aorta. Among 14 modules, the pink module exhibited the strongest correlation. **B,** Scatter plot illustrating the correlation between module membership (MM) and gene significance (GS) of each gene in the pink module. **C,** TOM plot of 78 genes with high MM and GS.

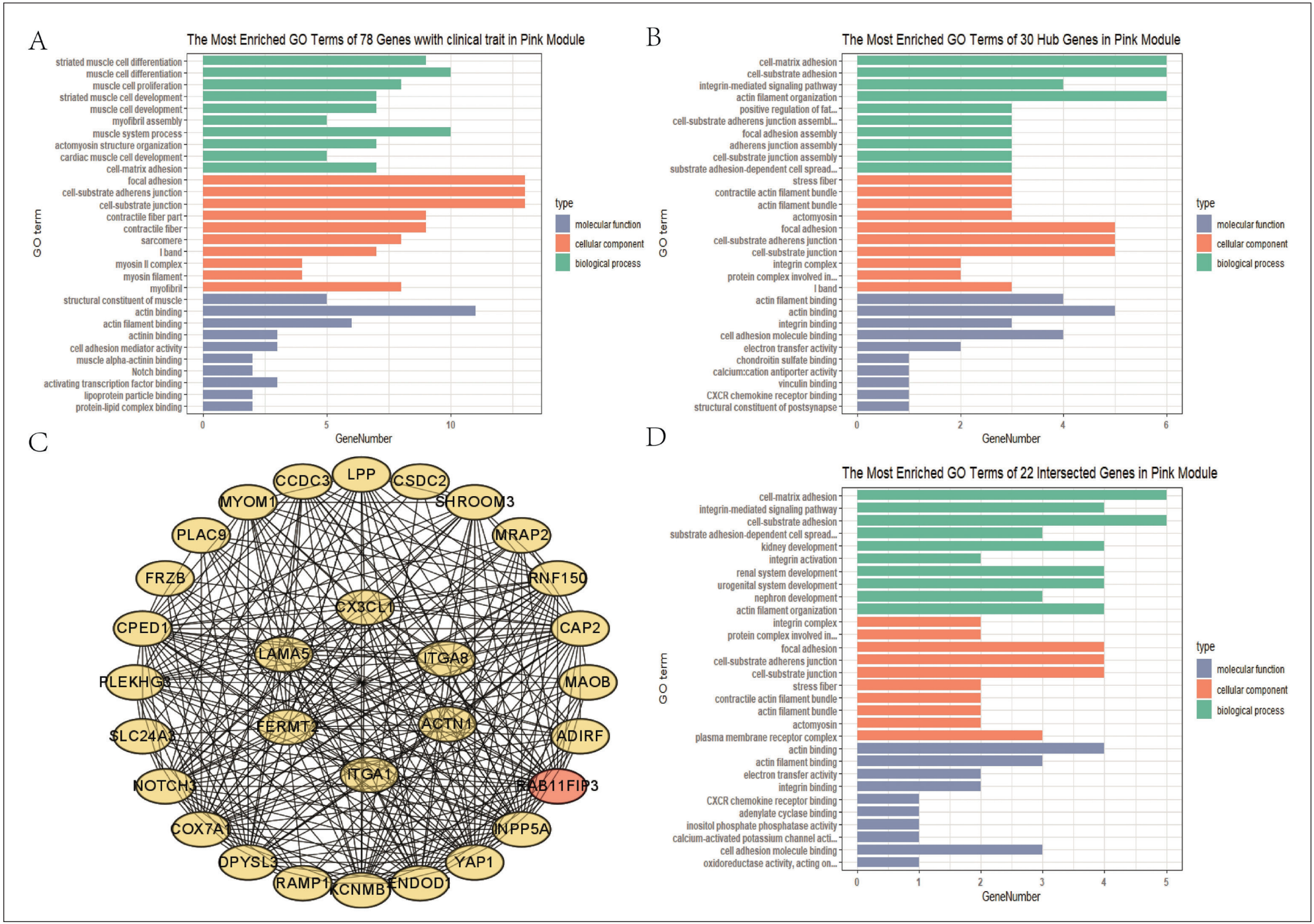

Figure 5. A, GO functional enrichment analyses of 78 genes with high MM and GS in pink module. **B,** GO functional enrichment analysis of the top 30 hub genes in pink module. **C,** Co-expression network of the top 30 hub genes in the pink module. **D,** GO functional enrichment analyses of 22 mutual genes with high MM and GS in pink module.

30 hub genes. Follow-up enrichment analyses on these 22 genes agreed with previous results from analysis of the hub genes (Figure 5D).

Analyses showed aberrant expression of genes relating to muscle cell proliferation, differentiation, and growth. This is in agreement with AAA pathology, which includes the atrophy and apoptosis of vascular smooth muscle. Furthermore, genes with high clinical significance and high network centrality were associated with the integrin-mediated signaling pathway and cell-matrix adhesion, indicating the potential involvement of both pathways in AAA pathogenesis.

Hub genes enriched in cell-matrix adhesion included *LAMA5, ACTN1, CX3CL1, ITGA8, ITGA1,* and *FERMT2*. Moreover, genes enriched in the integrin-mediated signaling pathway included *LAMA5, ITGA8, ITGA1,* and *FERMT2*. We observed a significant overlap between these two functional clusters, suggesting that the integrin-mediated signaling pathway may be involved in activation of focal adhesion, or in other words, the activation of cell-matrix adhesion. However, it is important to note that direct evidence implicating these genes in AAA formation is currently lacking. AUC values of *LAMA5, ACTN1, CX3CL1, ITGA8, ITGA1,* and *FERMT2* were plotted, and all found to be above 0.7 (Figure 6). Consequently, we selected these genes for subsequent experimental validation.

Validation in the Mouse Model of AAA

We successfully generated a mouse model of AAA with enlarged abdominal aorta exceeding 50% (Figure 7A). This model mimicked the main pathological and morphological features of human AAA. For instance, destruction of arterial elastic layer and apoptosis of smooth muscle cells. Expression levels of corresponding genes were: *LAMA5 = 0.068, p = 0.01, n = 3*; *ACTN1* = 0.22, *p* = 0.043, n = 4; *IGTA8* = 0.156, *p* = 0.010, n = 4; *IGTA1* = 0.22, *p* = 0.030, n = 4; *FERMT2 = 0.11, p = 0.032*, n = 3; *CX3CL* = 4.15, *p* = 0.016, n = 4 (Figure 7B). Low expression of *LAMA5, ACTN1, ITGA8, ITGA1,* and *FERMT2* in mouse AAA tissue was successfully verified at the mRNA level compared to normal abdominal aorta tissue. However, the expression level of *CX-3CL* is the opposite of the level suggested by the sequencing data (logFC = -0.603, *adj.p* = 0.011)

Discussion

Based on the GSE47472 and GSE57691 datasets, we conducted differential expression analysis, weighted gene co-expression network analysis, and functional enrichment analysis. From this, we successfully constructed 14 co-expression network modules. We found that the pink module showed the strongest correlation with AAA. As such, this was identified as the key module, and 30 hub genes were screened out from the pink module. Subsequently, 22 genes out of 30 hub genes showed high clinical significance. Among them, *LAMA5, ACTN1, CX3CL1, ITGA8, ITGA1*, and *FERMT2* were enriched in the integrin-mediated signaling pathway and cell-matrix adhesion. Furthermore, these genes showed a high predictive value. With the exception of *CX3CL1*, the low expression of *LAMA5, ACTN1, ITGA8, ITGA1,* and *FERMT2* were later verified in the mouse AAA model. Thus, based on these data, we hypothesize that inactivation of the integrin-mediated signaling pathway and cell-matrix adhesion may be implicated in AAA formation.

Summary of LAMA5, ACTN1, ITGA8, ITGA1, and FERMT2

LAMA5 (laminin α5) is an extracellular matrix glycoprotein in the basement membrane and is involved in mediating migration, growth, and differentiation of various cell types and cell-matrix adhesion. Deletion mutations in *LAMA5* can inhibit the β1 integrin signaling pathway through atypical kinase Pyk2 and Src kinases, thereby impairing focal adhesion formation[15].

ACTN1 encodes α-actinin-1, a cytoskeletal protein belonging to the filamentous actin (F-actin) crosslinking protein family[16]. In addition, α-actinin-1 is expressed at cell-matrix adhesion sites, cellular protrusions, and stress fiber dense regions and acts to bridge cytoskeleton and adhesion proteins[17]. Further, α-actinin-2 (*ACTN2*) and -3 (*ACTN3*) are subtypes specifically expressed in skeletal muscle cells. Studies have shown that *ACTN1,* which is widely expressed in various cells, is anchored to muscle cell membranes and is enriched in the ends of microfilament bundles[18]. *ACTN1* also bridges the cadherin–catenin complex to cytoskeletal actin[19]. Some clinical studies[20,21] revealed that *ACTN1* expression is associated with tumor proliferation and metastasis by suppressing the Hippo signaling pathway.

FERMT2 encodes integrin interacting protein 2 (kindlin-2), which is localized on cell-matrix adhesion sites[22]. The kindlins family is characterized by a C-terminal FERM domain. Kindlin-binding proteins (e.g., integrin-linked kinase (ILK), migfilin, integrin, and talin) are essential components in cell-matrix adhesion. On the cytoplasmic side, kindlin-2 directly binds to cytoplasmic tails of

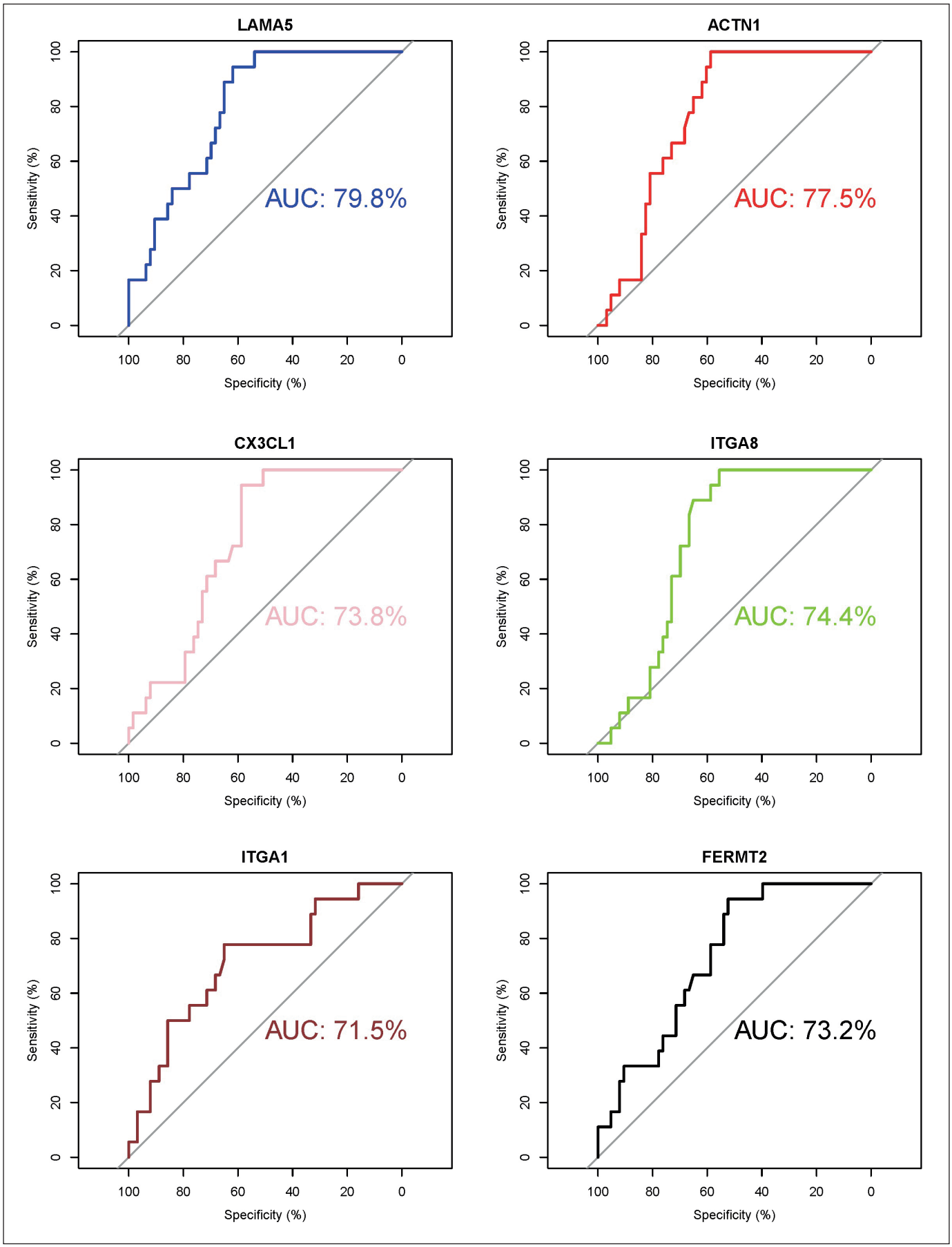

Figure 6. ROC curve of six genes related to the integrin signaling pathway and cell-matrix adhesion. All six genes had AUC values above 0.7.

the integrin β subunit and activates integrin under synergistic interaction with talin[23-25]. Kindlin-2 can also activate the outside/inside integrin pathway by recruiting paxillin to the junction of the cytoplasm and membrane, eventually initiating focal adhesion (FA) assembly[26]. Consequently, kindlin-2 can facilitate cytoskeletal reorganization caused by cell-matrix adhesion. Furthermore, *FERMT2* is highly expressed in non-small cell carcinoma. Studies have shown that *FERMT2* promotes invasion and metastasis of cancer cells via upregulation of cell adhesion[27]. *FERMT2* is also thought to play key roles in muscle development and can regulate muscle cell differentiation through the Wnt/β-catenin signaling pathway. Knockdown of kindlin-2 in endothelial cells results in impaired integrin-mediated cell-matrix adhesion to fibrinogen and vitronectin. Knockdown of *FERMT2* can lead to reduced expression of *Myh11*, *α-SMA*, and *CNN*, resulting in myofibril shortening, myofibril rupture, and decreased smooth muscle contractility[28].

CX3CL1 is a membrane-bound chemokine that mediates cell–cell adhesion, cell-matrix adhesion, as well as the immune/inflammatory response[29,30]. As an adhesion molecule, *CX3CL1* regulates adhesion of immune cells to vascular endothelial cells, thereby activating inflammatory response. This provides a plausible explanation for the inconsistency we observed between *CX3CL1* expression in human sequencing data and murine specimens. Seven days after elastase treatment, the abdominal aorta of mice in this study was still in the acute inflammatory phase, while the human AAA specimens were in the chronic inflammatory phase.

Integrins and Cell Adhesion

Integrins play major roles in cell-matrix adhesion[31]. Integrin-mediated cell-matrix adhesion

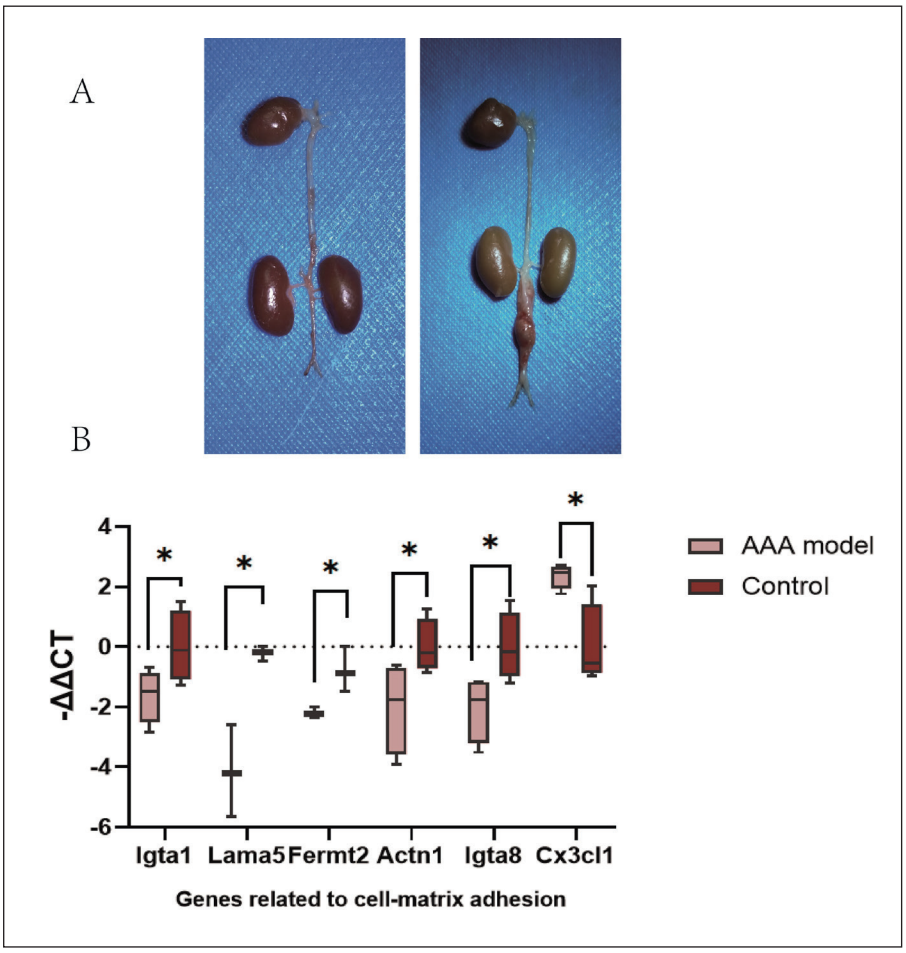

Figure 7. A, Mouse elastase-induced AAA model (right) and normal aorta from sham group (left). **B,** qPCR confirmed low expression of *IGTA1, LAMA5, FE2, ACTN1*, and *IGTA8* ($p < 0.05$). In contrast to the sequencing profile, *CX3CL1* expression was upregulated in mouse AAA tissue.

can provide support for the maintenance of vascular morphology[32]. Being composed of various adhesion proteins, integrin adhesion complexes (IACs) include focal complexes, FAs, and fibrillar adhesions[33]. IACs bind to cell membrane jointing ECM-bound integrins and intracellular cytoskeletal filaments. As α/β-heterodimeric transmembrane receptors, the integrin family consists of an intracellular tail domain and extracellular ligand-binding domain[34]. In the resting state, the ligand-binding sites of integrin are covered by two subunits, contributing to a low-affinity state. After being activated by internal or external signals, conformational changes are induced in integrin thoroughly exposing the ligand-binding sites, transforming it into a high-affinity state. The strong binding between integrins and ECM glycoproteins (e.g., fibronectins, collagens, and laminins) help to maintain stable cell adhesion[34]. Further, activated integrins interact with the FERM domain of focal adhesion kinase (FAK), triggering FAK phosphorylation and FA assembly.

Potential Roles of FA and Cell-Matrix Adhesion in AAA Formation

Cell stiffness and adhesion characteristics of VSMC are thought to be significant factors involved in the maintenance of overall artery stiffness[35]. Adhesive force refers to the strength required to break the probe binding ECM proteins and cell membranes. VSMC-ECM adhesion involves collagen, elastin, adhesion proteins, integrin receptors, and FA. In the ECM, in combination with actomyosin of the smooth muscle cytoskeleton, integrin and FA are the most important structures in the VSMC-ECM interaction. Proteomic investigations have shown that high expression of cytoskeleton and FA complexes in vascular smooth muscle led to increased elasticity in the thoracic aorta. A decrease in FA sites reduces the stiffness of the abdominal aortic wall, thereby contributing to aortic dilations.

We assume that low expression of adhesion molecules may break the tight junction between endothelial cells. In this case, inflammatory cells in circulation can then migrate to and accumulate in the extracellular matrix. The reduction in the interconnection between VSMCs also promotes dilation of aortae under high blood pressure leading to formation of an aneurysm. Biros et al[36] reported transcriptome sequencing data of 49 AAA samples, 9 AOD samples, and 10 normal aorta samples. The authors conducted KEGG pathway enrichment analysis for up- and downregulated genes. Highly expressed genes in AAA were found to be enriched in immune-related pathways (interaction of cytokines and cytokine receptors, chemokine signaling pathways, and T cell receptor signaling pathways), indicating an overactive immune response and immune cell recruitment. The downregulated genes were enriched in metabolic pathways, FA, and smooth muscle contraction, indicating a limited smooth muscle cell contractility. The upregulated expression of *CTLA4, NKTR*, and *CD8a* was further confirmed by qPCR. In addition, *CTLA4* was highly expressed in small-diameter human AAA, while *CD8a* was highly expressed in large-diameter human AAA. *NKTR* was highly expressed in both small- and large-diameter AAA.

Conclusions

The key genes in the integrin-mediated signaling pathway that regulates the cell-matrix (*LAMA5, ACTN1, ITGA8, ITGA1,* and *FERMT2*) are downregulated in AAA. The loss of cell-matrix adhesion reduces the stiffness of the abdominal aortic wall, which contributes to aortic dilations.

Data Availability

The datasets used and analyzed in the current study are available from the public Gene Expression Omnibus database (https://www.ncbi.nlm.nih.gov).

Funding

This study is supported by Scientific research project of Shanxi Provincial Health Commission (grant number: 2022053).

Conflicts of Interest

The authors declare no conflicts of interest.

Acknowledgments

We acknowledge GEO databases for providing their platforms and contributors for uploading their meaningful datasets.

Ethical Approval

The study has been approved by Ethics Committee of the Second Hospital of Shanxi Medical University (No. DW2022003).

References

1) Johnston KW, Rutherford RB, Tilson MD, Shah DM, Hollier L, Stanley JC. Suggested standards

for reporting on arterial aneurysms. Subcommittee on Reporting Standards for Arterial Aneurysms, Ad Hoc Committee on Reporting Standards, Society for Vascular Surgery and North American Chapter, International Society for Cardiovascular Surgery. J Vasc Surg 1991; 13: 452-458.

2) Lederle FA. Ultrasonographic screening for abdominal aortic aneurysms. Ann Intern Med 2003; 139: 516-522.

3) Investigators IT. Comparative clinical effectiveness and cost effectiveness of endovascular strategy v open repair for ruptured abdominal aortic aneurysm: three year results of the IMPROVE randomised trial. BMJ 2017; 359: j4859.

4) Lederle FA. The rise and fall of abdominal aortic aneurysm. Circulation 2011; 124: 1097-1099.

5) Michel JB, Martin-Ventura JL, Egido J, Sakalihasan N, Treska V, Lindholt J, Allaire E, Thorsteinsdottir U, Cockerill G, Swedenborg J. Novel aspects of the pathogenesis of aneurysms of the abdominal aorta in humans. Cardiovasc Res 2011; 90: 18-27.

6) Koch AE, Haines GK, Rizzo RJ, Radosevich JA, Pope RM, Robinson PG, Pearce WH. Human abdominal aortic aneurysms. Immunophenotypic analysis suggesting an immune-mediated response. Am J Pathol 1990; 137: 1199-1213.

7) Li Y, Wang W, Li L, Khalil RA. MMPs and ADAMs/ADAMTS inhibition therapy of abdominal aortic aneurysm. Life Sci 2020; 253: 117659.

8) Vorkapic E, Folkesson M, Magnell K, Bohlooly YM, Länne T, Wågsäter D. ADAMTS-1 in abdominal aortic aneurysm. PLoS One 2017; 12: e0178729.

9) Kawai T, Takayanagi T, Forrester SJ, Preston KJ, Obama T, Tsuji T, Kobayashi T, Boyer MJ, Cooper HA, Kwok HF, Hashimoto T, Scalia R, Rizzo V, Eguchi S. Vascular ADAM17 (a Disintegrin and Metalloproteinase Domain 17) Is Required for Angiotensin II/β-Aminopropionitrile-Induced Abdominal Aortic Aneurysm. Hypertension 2017; 70: 959-963.

10) Muratoglu SC, Belgrave S, Hampton B, Migliorini M, Coksaygan T, Chen L, Mikhailenko I, Strickland DK. LRP1 protects the vasculature by regulating levels of connective tissue growth factor and HtrA1. Arterioscler Thromb Vasc Biol 2013; 33: 2137-2146.

11) Davis FM, Rateri DL, Balakrishnan A, Howatt DA, Strickland DK, Muratoglu SC, Haggerty CM, Fornwalt BK, Cassis LA, Daugherty A. Smooth muscle cell deletion of low-density lipoprotein receptor-related protein 1 augments angiotensin II-induced superior mesenteric arterial and ascending aortic aneurysms. Arterioscler Thromb Vasc Biol 2015; 35: 155-162.

12) Angelov SN, Hu JH, Wei H, Airhart N, Shi M, Dichek DA. TGF-β (Transforming Growth Factor-β) Signaling Protects the Thoracic and Abdominal Aorta From Angiotensin II-Induced Pathology by Distinct Mechanisms. Arterioscler Thromb Vasc Biol 2017; 37: 2102-2113.

13) Langfelder P, Horvath S. WGCNA: an R package for weighted correlation network analysis. BMC Bioinformatics 2008; 9: 559.

14) Yu G, Wang LG, Han Y, He QY. clusterProfiler: an R package for comparing biological themes among gene clusters. Omics 2012; 16: 284-287.

15) Barad M, Csukasi F, Bosakova M, Martin JH, Zhang W, Paige Taylor S, Lachman RS, Zieba J, Bamshad M, Nickerson D, Chong JX, Cohn DH, Krejci P, Krakow D, Duran I. Biallelic mutations in LAMA5 disrupts a skeletal noncanonical focal adhesion pathway and produces a distinct bent bone dysplasia. EBioMedicine 2020; 62: 103075.

16) Oikonomou KG, Zachou K, Dalekos GN. Alpha-actinin: a multidisciplinary protein with important role in B-cell driven autoimmunity. Autoimmun Rev 2011; 10: 389-396.

17) Otey CA, Carpen O. Alpha-actinin revisited: a fresh look at an old player. Cell Motil Cytoskeleton 2004; 58: 104-111.

18) Wehland J, Osborn M, Weber K. Cell-to-substratum contacts in living cells: a direct correlation between interference-reflexion and indirect-immunofluorescence microscopy using antibodies against actin and alpha-actinin. J Cell Sci 1979; 37: 257-273.

19) Knudsen KA, Soler AP, Johnson KR, Wheelock MJ. Interaction of alpha-actinin with the cadherin/catenin cell-cell adhesion complex via alpha-catenin. J Cell Biol 1995; 130: 67-77.

20) Xie GF, Zhao LD, Chen Q, Tang DX, Chen QY, Lu HF, Cai JR, Chen Z. High ACTN1 Is Associated with Poor Prognosis, and ACTN1 Silencing Suppresses Cell Proliferation and Metastasis in Oral Squamous Cell Carcinoma. Drug Des Devel Ther 2020; 14: 1717-1727.

21) Chen Q, Zhou XW, Zhang AJ, He K. ACTN1 supports tumor growth by inhibiting Hippo signaling in hepatocellular carcinoma. J Exp Clin Cancer Res 2021; 40: 23.

22) Larjava H, Plow EF, Wu C. Kindlins: essential regulators of integrin signalling and cell-matrix adhesion. EMBO Rep 2008; 9: 1203-1208.

23) Shi X, Ma YQ, Tu Y, Chen K, Wu S, Fukuda K, Qin J, Plow EF, Wu C. The MIG-2/integrin interaction strengthens cell-matrix adhesion and modulates cell motility. J Biol Chem 2007; 282: 20455-20466.

24) Ma YQ, Qin J, Wu C, Plow EF. Kindlin-2 (Mig-2): a co-activator of beta3 integrins. J Cell Biol 2008; 181: 439-446.

25) Calderwood DA, Campbell ID, Critchley DR. Talins and kindlins: partners in integrin-mediated adhesion. Nat Rev Mol Cell Biol 2013; 14: 503-517.

26) Zhu L, Liu H, Lu F, Yang J, Byzova TV, Qin J. Structural Basis of Paxillin Recruitment by Kindlin-2 in Regulating Cell Adhesion. Structure 2019; 27: 1686-1697.e1685.

27) Guo WH, Bian JJ, Tian GF, Lyu ZX, Gui YX, Ye L. [Expression of Fermintin family homologous protein 2 in non-small cell lung cancer and its clinical significance]. Zhonghua Bing Li Xue Za Zhi 2018; 47: 780-783.

28) He X, Song J, Cai Z, Chi X, Wang Z, Yang D, Xie S, Zhou J, Fu Y, Li W, Kong W, Zhan J, Zhang H.

Kindlin-2 deficiency induces fatal intestinal obstruction in mice. Theranostics 2020; 10: 6182-6200.

29) Imai T, Yasuda N. Therapeutic intervention of inflammatory/immune diseases by inhibition of the fractalkine (CX3CL1)-CX3CR1 pathway. Inflamm Regen 2016; 36: 9.

30) Ferretti E, Pistoia V, Corcione A. Role of fractalkine/CX3CL1 and its receptor in the pathogenesis of inflammatory and malignant diseases with emphasis on B cell malignancies. Mediators Inflamm 2014; 2014: 480941.

31) Lietha D, Izard T. Roles of Membrane Domains in Integrin-Mediated Cell Adhesion. Int J Mol Sci 2020; 21.

32) Khan RB, Goult BT. Adhesions Assemble!-Autoinhibition as a Major Regulatory Mechanism of Integrin-Mediated Adhesion. Front Mol Biosci 2019; 6: 144.

33) Humphries JD, Chastney MR, Askari JA, Humphries MJ. Signal transduction via integrin adhesion complexes. Curr Opin Cell Biol 2019; 56: 14-21.

34) Li Z, Lee H, Zhu C. Molecular mechanisms of mechanotransduction in integrin-mediated cell-matrix adhesion. Exp Cell Res 2016; 349: 85-94.

35) Lacolley P, Regnault V, Segers P, Laurent S. Vascular Smooth Muscle Cells and Arterial Stiffening: Relevance in Development, Aging, and Disease. Physiological Reviews 2017; 97: 1555-1617.

36) Biros E, Gäbel G, Moran CS, Schreurs C, Lindeman JH, Walker PJ, Nataatmadja M, West M, Holdt LM, Hinterseher I, Pilarsky C, Golledge J. Differential gene expression in human abdominal aortic aneurysm and aortic occlusive disease. Oncotarget 2015; 6: 12984-12996.